Iraqi Journal of Physics, 2026 *Vol.24, No.3, PP.101-112*
https://doi.org/10.30723/ijp.v24i3.1506 *P-ISSN: 2070-4003*
E-ISSN: 2664-5548

Theoretical Study of the Nuclear Structure for Some Exotic Nuclei (^{9}C, ^{23}Al and ^{27}P) using Unitary Correlation Operator Method

Saja Kh. Abdulrazaq[1*] and Ghaith N. Flaiyh[1]
[1]*Department of Physics, College of Science, University of Baghdad, Baghdad, Iraq*
[*]Corresponding author: saja.abd2404m@sc.uobaghdad.edu.iq

Abstract
The nuclear structure of some one-proton exotic nuclei (^{9}C, ^{23}Al and ^{27}P) was investigated using the Unitary Correlation Operator Method (UCOM). The nuclei were divided into two regions: the core and the valence nucleons. A transformation from the one-body to the two-body framework was applied, incorporating the correlation operator (C), which accounts for both tensor correlations (C_{Ω}) and short-range central correlations (C_r). The density distributions for each region were then computed separately, and the total density was determined. From this, the expectation value of the density was calculated, leading to the determination of the mean square radius $\langle r^2 \rangle^{1\backslash 2}$. The Plane Wave Born Approximation (PWBA) was used to study these nuclei for elastic electron scattering. Based on the computed results, it was found that this model provides an accurate and reliable description of the nuclear structure of the studied halo nuclei. A comparison between the calculated values of the mean square radius and experimental data demonstrated strong agreement, confirming the validity of the approach for describing the structure of halo nuclei.

Article Info.

Keywords:
Exotic Nuclei, Density Distribution, Unitary Correlation Operator Method (UCOM), Root Mean Square Radius (RMS), Plane Wave Born Approximation (PWBA).

Article history:
Received: Jul. 26, 2025
Revised: Oct. 21, 2025
Accepted: Nov. 14, 2025
Published: Sep.01, 2026

1. Introduction

Halo nuclei are recognized as a distinct class of atomic nuclei found in proximity to the nuclear drip line. These nuclei are characterized by the presence of one or two nucleons (most often neutrons, and occasionally protons) that are very weakly bound to a dense central core. The wave function of the loosely coupled nucleons is significantly extended spatially as a result of this weak binding, creating a widely diffused "halo" of nuclear matter that extends considerably beyond the traditional boundaries of the nucleus. This phenomenon is a direct consequence of the low binding energy, which allows these nucleons to traverse much larger distances within the nuclear potential, thereby forming a nuclear structure with an effective radius significantly larger than expected based on their total nucleon count [1, 2].

The investigation of exotic nuclei, particularly those with a significant proton excess, has attracted considerable interest because of their distinctive structural characteristics, such as the formation of proton halos. These properties pose a significant challenge to conventional nuclear models, thus necessitating the adoption of advanced theoretical methodologies to ensure an accurate representation of nuclear structure. The Unitary Correlation Operator Method (UCOM) stands out as one such approach, distinguished by its efficacy in representing short-range and tensor interactions within the nucleus [3, 4].

Recent theoretical investigations have examined the nuclear structure of proton-rich halo nuclei, which are characterized by an expansion of their peripheral nuclear density. Hammoudi et al. found a proton halo in the ^{17}Ne and ^{27}P nuclei, which were obtained using elastic electron scattering data and a two-frequency shell model. The usual long-tail behavior in proton density distinguishes this halo structure [5]. Hansen et al. studied the halo structure of (17Ne and 27P) using the two-frequency shell model. They calculated the nuclear density distributions, rms radii, and elastic electron-scattering form factors using PWBA. Their results confirmed the proton-halo structure of both nuclei [6]. Hussein and Flaiyh studied the proton-rich nuclei 23Al and 27P using two-body charge density distributions (2BCDDs) within the two-frequency shell model. They investigated the nuclear density distributions, rms radii, and elastic electron-scattering form factors using PWBA. Their results confirmed the proton-halo structure of both nuclei, with good agreement between the calculated and experimental results [7]. Related work by Issa and Flaiyh studied the charge density distributions of 20Ne and 24Mg using the folding model and two-body density distributions. They calculated the elastic and inelastic electron-scattering form factors and rms charge radii. Their results showed good agreement between the calculated inelastic form factors and the experimental data, highlighting the importance of core polarization effects [8]. Additionally, Neff and Feldmeier introduced the Unitary Correlation Operator Method (UCOM) to incorporate short-range two-body correlations arising from the strong repulsive core and tensor part of the nucleon–nucleon interaction into shell-model states. They showed that UCOM can be applied within mean-field and shell-model spaces to account for these correlations [9]. Abbas and Flaiyh conducted a study on the stable nuclei ^{19}F and ^{27}Al using the UCOM. The research focused on short-range nuclear correlations and their effects on electron scattering form factors, charge density distributions, and rms radii. The experimental data correlated well with the results, proving that this approach properly studies nuclear structure [10].

This work uses UCOM to study the nuclear structure of a few one-proton halo nuclei, including the isotopes of (^{9}C, ^{23}Al, and ^{27}P), to separate core and valence nucleon contributions, and to calculate matter density distributions; the one-body density operator must be turned into a two-body framework. This study aims to determine the exotic nuclei matter density, elastic electron scattering form factors, and rms radii. Additionally, the theoretical findings will be compared with the available experimental observations to assess their consistency.

2. Theory

The nucleon density distribution is divided into two parts: the first corresponds to the core nucleons, while the second is associated with the valence (halo) nucleons. Therefore, the total nucleon density distribution for a halo nucleus is expressed as follows [11]:

$$\rho_{matt}(r) = \rho_{core}^{p+n}(r) + \rho_{valence}^{p(n)}(r) \quad \textbf{(1)}$$

where ρ is the nuclear density distribution, ρ_{core} is the core (inner) nucleon density, and ρ_{valence} is the valence or halo nucleon density. The one-body density operator [12]:

$$\hat{\rho}^{(1)}(\vec{r}) = \sum_{i=1}^{A} \delta(\vec{r} - \vec{r}_i) \quad \textbf{(2)}$$

where $\vec{r}$ is the radial distance from the center of the nucleus; ρ_{core} (r) and ρ_{valence} (r) represent the density contributions from the core and valence nucleons, respectively.

$$\sum_{i=1}^{A} \delta(\vec{r} - \vec{r}_i) \equiv \frac{1}{2(A-1)} \sum_{i\neq j} \left\{ \delta(\vec{r} - \vec{r}_i) + \delta(\vec{r} - \vec{r}_j) \right\} \quad \textbf{(3)}$$

A useful transformation can be performed by converting the two-particle $\vec{r_i}$ and $\vec{r_j}$ coordinates into the relative $\overrightarrow{r_{ij}}$ and center-of-mass $\overrightarrow{R_{ij}}$ coordinates[13]:

$$\vec{r}_i = \frac{1}{\sqrt{2}}(\vec{R}_{\text{ij}} + \vec{r}_{\text{ij}}) \quad \textbf{(4-a)}$$

$$\vec{r}_j = \frac{1}{\sqrt{2}}(\vec{R}_{\text{ij}} - \vec{r}_{\text{ij}}) \quad \textbf{(4-b)}$$

Introducing Eqs. (4-a) and (4-b) into Eq. (3) yields:

$$\hat{\rho}(2)\,(\vec{r}) = \frac{\sqrt{2}}{(A-1)}\,\sum_{i\neq j}\left\{\delta\left[(2)^{1l2}\vec{r}-\vec{R}_{\mathrm{ij}}-\vec{r}_{\mathrm{ij}}\right]+\delta\left[(2)^{1l2}\vec{r}-\vec{R}_{\mathrm{ij}}+\vec{r}_{\mathrm{ij}}\right]\right\} \quad \textbf{(5-a)}$$

Using the identity:

$$\delta(a\vec{r}) = \frac{1}{|a^3|}\delta(\vec{r}) \quad \textbf{(5-b)}$$

By applying the relevant identity Eq. (5-b), Eq. (5-a) can be reformulated into the following expression for further analysis:

$$\hat{\rho}(2)\quad(\vec{r}) = \frac{\sqrt{2}}{2(A-1)}\,.\sum_{i\neq j}\left\{\delta\left[\sqrt{2}\vec{r}-\vec{R}_{\mathrm{ij}}-\vec{r}_{\mathrm{ij}}\right]+\delta\left[\sqrt{2}\vec{r}-\vec{R}_{\mathrm{ij}}+\vec{r}_{\mathrm{ij}}\right]\right\} \quad \textbf{(6)}$$

An effective nucleon density operator, suitable for use with uncorrelated wave functions, can be constructed by convoluting the operator defined in Eq. (5) with the two-body correlation functions, denoted as C:

$$\hat{\rho}(2)_{eff}(\vec{r}) = \frac{\sqrt{2}}{2(A-1)}\,\sum_{i\neq j}C\left\{\delta\left[\sqrt{2}\vec{r}-\vec{R}_{\mathrm{ij}}-\vec{r}_{\mathrm{ij}}\right]+\delta\left[\sqrt{2}\vec{r}-\vec{R}_{\mathrm{ij}}+\vec{r}_{\mathrm{ij}}\right]\right\}C \quad (7)$$

where the correlation operator C is described as:

$$C = C_\Omega C_r \quad \textbf{(8)}$$

where C_r is the central correlation short-range, and C_Ω is the tensor correlation. Each of these unitary operators is expressed with Hermitian two-body generators [14, 15]:

$$\left.\begin{aligned} C_r &= exp\left[-i\sum_{i<j}g_{r,ij}\right]\\ C_\Omega &= exp\left[-i\sum_{i<j}g_{\Omega,ij}\right]\end{aligned}\right\} \quad \textbf{(9)}$$

where g_r is the generator of the central correlation operator and g_Ω is the generator of the tensor correlation operator, which will rely on the particular NN interaction [14]. The generator for the central correlation is expressed as follows:

$$g_r = \sum_{S.T}\frac{1}{2}\left[q_r S_{ST(r)} + S_{ST}(r)q_r\right]\Pi_{ST} \quad \textbf{(10)}$$

where Π_{ST} is the dropping operator onto two-body spin S and isospin T. For a two-body system, transform using a numerically known correlation function $R_+(r)$. Thus, the numerically specified $R_+(r)$ was parameterized [14, 15]:

$$R_+(r) = r + \alpha\left(\frac{r}{\beta}\right)^\eta exp\left\{-\,exp\left(\frac{r}{\beta}\right)\right\} \quad \textbf{(11)}$$

The parameter α governs the magnitude of the shift, β sets the spatial scale, while η influences the sharpness of the variation near r = 0. These parameters are used in the central correlation function to define the strength, range, and sharpness of the short-range correlations in the UCOM method.

In a Hermitized form, the complete generator for the tensor correlations is expressed as follows:

$$g_\Omega = \sum_T \vartheta_T(r)\,S_{12}\left(\vec{r},\vec{q_\Omega}\right)\Pi_{1T} \quad \textbf{(12)}$$

Making use of the public definition for a rank 2 tensor operator:

$$S_{12}\left(\vec{a},\vec{b}\right) = \frac{3}{2}\left[\left(\vec{\sigma}.\vec{a}\right)\left(\vec{\sigma}.\vec{b}\right) + \left(\vec{\sigma}.\vec{b}\right)\left(\vec{\sigma}.\vec{a}\right)\right] - \frac{1}{2}\left(\vec{\sigma}.\vec{\sigma}\right)\left(\vec{a}.\vec{b} + \vec{b}.\vec{a}\right) \quad \textbf{(13)}$$

The amplitude is given by the tensor correlation function $\vartheta_T(r)$. The tensor correlation function $\vartheta_T(r)$ is represented using a specific parameterized form, tailored to capture the spatial characteristics of the tensor interaction within the nucleon-nucleon potential [13,14]:

$$\vartheta(r) = \alpha\left[1 - exp\left(-\frac{r}{\gamma}\right)\right] exp\left[-exp\left(\frac{r}{\beta}\right)\right] \quad \textbf{(14)}$$

In the case of closed-shell nuclei, the Two-Body Nucleon Density Distribution (2BNDD) is derived from the expectation value of the correlated two-body charge density operator, as defined in Eq. (7), and is formally represented as follows:

$$\rho_o(r) = \left\langle \Psi | \hat{\rho}^{(2)}_{eff}\left(\vec{r}\right) | \Psi \right\rangle = \sum_{i<j} \left\langle ij | \hat{\rho}^{(2)}_{eff}\left(\vec{r}\right)\left[|ij\rangle - |ji\rangle\right]\right\rangle \quad \textbf{(15)}$$

where ψ is the nuclear wave function.

The two-particle wave function is given by [16]:

$$|ij\rangle = \sum_{JM_J}\sum_{TM_T} \left\langle j_i m_i\, j_j m_j \middle| JM_J \right\rangle \left\langle t_i m_{t_i}\, t_j m_{t_j} \middle| TM_T \right\rangle \left|(j_i\, j_j)JM_J\right\rangle \left|(t_i t_j)TM_T\right\rangle \quad \textbf{(16)}$$

It should be noted that the correlated two-body charge density operator introduced in Eq. (7) is formulated in terms of relative and center-of-mass coordinates. Consequently, the spatial and spin components of the two-particle wave function, originally expressed in the jj-coupling representation, must be appropriately transformed into the relative and center-of-mass coordinate systems to ensure consistency within this framework [16]. The rms radii corresponding to the above density are given by [17]:

$$\left\langle r^2 \right\rangle^{1/2}_W = \frac{4\pi}{W}\int_0^\infty \rho^W(r)\, r^4 dr \quad \textbf{(17)}$$

In the Plane-Wave Born Approximation (PWBA), both the incoming and outgoing electron wave functions are approximated as ideal plane waves. This simplifies the interaction analysis between the electron and the nuclear target. In the case of spin-zero nuclei with a real and spherically symmetric charge density distribution in the ground state, the elastic electron scattering form factor, F(q), can be directly obtained from the Fourier transform of this distribution. Mathematically, the form factor is given by the following expression [18, 19]:

$$F(q) = \frac{4\pi}{z}\int_0^\infty \rho_m(r) j_o(qr) r^2 dr \quad \textbf{(18)}$$

where$j_o(qr) = sin(qr)/(qr)$ represents the spherical Bessel function of order zero, and q denotes the momentum transferred from the incoming electron to the target nucleus. Accordingly, Eq. (18) can be reformulated in the following manner:

$$F(q) = \frac{4\pi}{qz}\int_0^\infty \rho_0\,(r)\, sin(qr)\, r dr \quad \textbf{(19)}$$

where F(q) is the total form factor, F_{fs}(q) is the finite-size correction of the nucleon and F_{cm} (q) represents the center-of-mass correction.

$$F_{fs}(q) = e^{-0.43q^2\backslash 4} \quad \textbf{(20)}$$

$$F_{cm}(q) = e^{q^2 b^2 \backslash 4A} \quad \textbf{(21)}$$

By applying the corrections from Eqs. (20) and (21), the total form factor in Eq. (19) is obtained:

$$F(q) = \frac{4\pi}{qz}\int_0^\infty \rho_o\,(r)\,sin(qr)\,rdrF_{fs}(q)F_{cm}(q) \quad \textbf{(22)}$$

The above formalism provides the theoretical framework used to compute the density distributions, mean square radii, and elastic electron scattering form factors for the selected exotic nuclei.

3. Results and Discussion

The ground state characteristics of one-proton halo nuclei were evaluated using the UCOM. As part of the assessments, root-mean-square radii were calculated. To increase the precision of nuclear structure computations, distinct model spaces were used for the core and halo regions. The research used two different size parameters: the valence size parameter and the core size parameter. The parameters b_c, b_v, b_{matt}, α, β, and η were adjusted to reproduce the experimental rms radii of the studied nuclei, ensuring that the calculated densities and radii are consistent with the experimental data. These parameters, used in the nuclear structure analysis based on the UCOM method for the selected exotic nuclei, are listed in Table 1. The table also includes three additional parameters, α, β, and η, which are defined by Eqs. (11) and (14). These parameters are associated with the mathematical expressions of the short-range and tensor correlation functions ϑ(r) employed in the UCOM framework.

Table 1: The Parameters for b_c, b_v, and b_{matt} applied to the UCOM methodology of the present study to match the calculated and experimental rms radii of exotic nuclei (^{9}C, ^{23}Al, and ^{27}P).

Exotic Nuclei	Core Nuclei	b_c (fm)	b_y (fm)	b_m (fm)	α	β	η
C	^{8}B	1.83	2.54	2.04	1.20	1.15	0.095
^{23}Al	^{22}Mg	1.91	3.27	1.91	1.42	1.3	0.160
^{27}P	^{26}Si	1.92	3.21	2.00	1.47	1.33	0.25

The estimated and observed root-mean-square radii for these exotic nuclei show good agreement with experimental data, as shown in Table 2 [20–23]. The experimental error margins are all within or close to the computed values. This agreement shows that the ground state features of these unusual systems may be accurately described using the UCOM technique. The sensitivity of the parameters to the calculated rms radii was tested by varying each by ±5%. The resulting rms values changed by less than 2%, confirming that the parameters are well constrained by the experimental data. The graphs of Figs. 1-3 illustrate the relationship between nuclear matter density and the radial distance(r) from the center of the nucleus. The horizontal axis represents the distance from the nuclear center in femtometers (fm), while the vertical axis displays the nuclear matter density (ρ) in fm^{-3} on a logarithmic scale.

These figures include several key components: the red curve represents the shell model, which failed to reproduce the distinctive behavior of exotic nuclei. The blue curve shows the core density, which also failed to exhibit the long-tail behavior. The black curve indicates the valence proton density, and the green curve reflects the total matter density. The shaded gray region signifies the extended distribution of nuclear matter beyond the conventional nuclear boundary, highlighting the influence of the proton halo. This study focuses on three proton-rich isotopes that exhibit potential proton halo characteristics. These results are consistent with previous theoretical works by Hamoudi et al. [4] and Rahi and Flaiyh [21], which also reported extended density distributions in proton-rich nuclei.

Table 2: The calculated and experimental rms radii of exotic nuclei (^{9}C, ^{23}Al and ^{27}P).

Exotic Nuclei	Core Nuclei	RMS matter radius for core nuclei $< r^2 >^{1\backslash 2}_{core}$ (fm)		RMS matter radius for valence nuclei $< r^2 >^{1/2}_{matt}$ (fm)	
		Calculated Results	Experimental Results	Calculated Results	Experimental Results
^{9}C	^{8}B	2.47	2.38±0.04 [20]	2.75	2.75±0.34 [21]
^{23}Al	^{22}Mg	2.98	2.78±0.26 [22]	2.98	2.905±0.25 [22]
^{27}P	^{26}Si	3.11	3.03± .06 [23]	3.23	3.23± 0.13 [23]

3.1. ^{9}C Nucleus

Exotic nuclei with a single proton have short half-lives of 126.5 ms. The core (J^{π}, T= 1+,2) and the valence single proton (J_{π}, T= $\frac{1}{2}^{-}$, $\frac{3}{2}$) are coupled to create the nucleus (J^{π}, T= $\frac{3}{2}^{-}$, $\frac{3}{2}$). With an rms radius of 2.47 fm and an oscillator size parameter of b_c = 1.83 for the core, the results are consistent with the experimental value of 2.38 ± 0.04 fm. With an oscillator size parameter of b_m = 2.04 fm, the valence proton is assumed to inhabit a pure ($1p_{1\backslash 2}$) state with an rms radius of b_v = 2.88 fm, which is in agreement with the experimental finding of 2.75 ± 0.34 fm. Table 2 displays the estimated and observed nucleon rms radii for this nucleus. The experimental results and the theoretically determined values of rms radii show a strong correlation. Fig. 1 shows the plot of the ground-state 2BNDD in fm^{-3} as a function of r (in fm). The black line, which shows a long tail in this distribution, represents the valence contribution (one proton in the $1p_{1\backslash 2}$ state), while the blue line represents the core normal contribution. The green line, representing the matter density distribution (core + valence), has a large tail and closely matches the experimental data shown by the shaded region.

The elastic electron scattering form factors of ^{9}C nuclei are shown in Fig. 2. The red curve represents the theoretically calculated form factors for each ^{9}C nucleus. At the same time, the black dots correspond to the experimental data of their stable counterparts, ^{12}C. The calculated form factors for the proton-rich nuclei exhibit distinct behavior, characterized by a significant spatial extension of nucleon distributions, particularly for the valence neutrons.

This extended distribution provides strong evidence for the presence of neutron halo structures in these nuclei, in which weakly bound neutrons occupy orbitals far from the nuclear core. The noticeable deviation between the theoretical form factors and the experimental data for the stable nuclei further supports this interpretation. These findings highlight the importance of incorporating halo effects when modeling the nuclear structure of systems near the proton drip line.

3.2. ^{23}Al Nucleus

The one-proton exotic nucleus ^{23}Al has a short half-life of 0.47 seconds. The nucleus (J^{π}, T= $1\backslash 2^{+}$, 5/2) is generated by the coupling of the core (J^{π}, T= 0^{+}, 0) with the valence one-proton (J^{π}, T= $1/2^{+}$, 5/2). The oscillator size parameter for the core is b_c = 1.91, resulting in an rms radius of 2.98 fm, which aligns with the experimental value of 2.78 ± 0.26 fm. The valence proton is assumed to occupy a pure ($2s_{1\backslash 2}$) state with an oscillator size parameter of b_v = 3.27 fm; using b_{matt} = 1.91 yields an rms radius of 2.94 fm, consistent with the experimental result of 2.905 ± 0.25 fm.

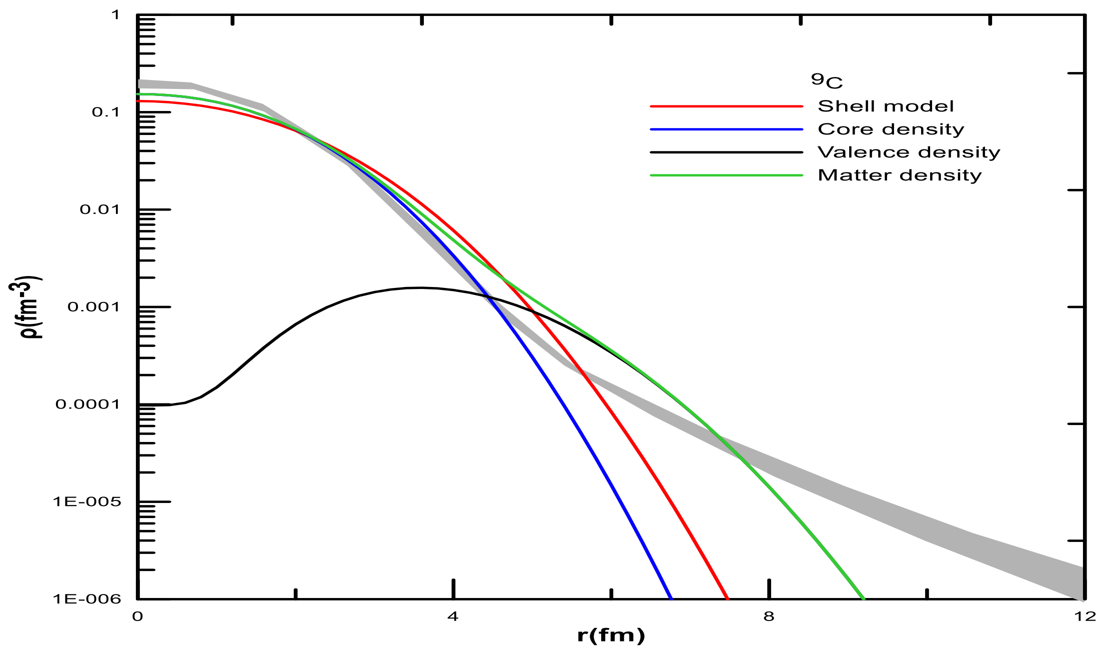

Figure 1: Calculated matter density distribution for ^{9}C with UCOM parameters compared with the fit to the experimental data [21,22].

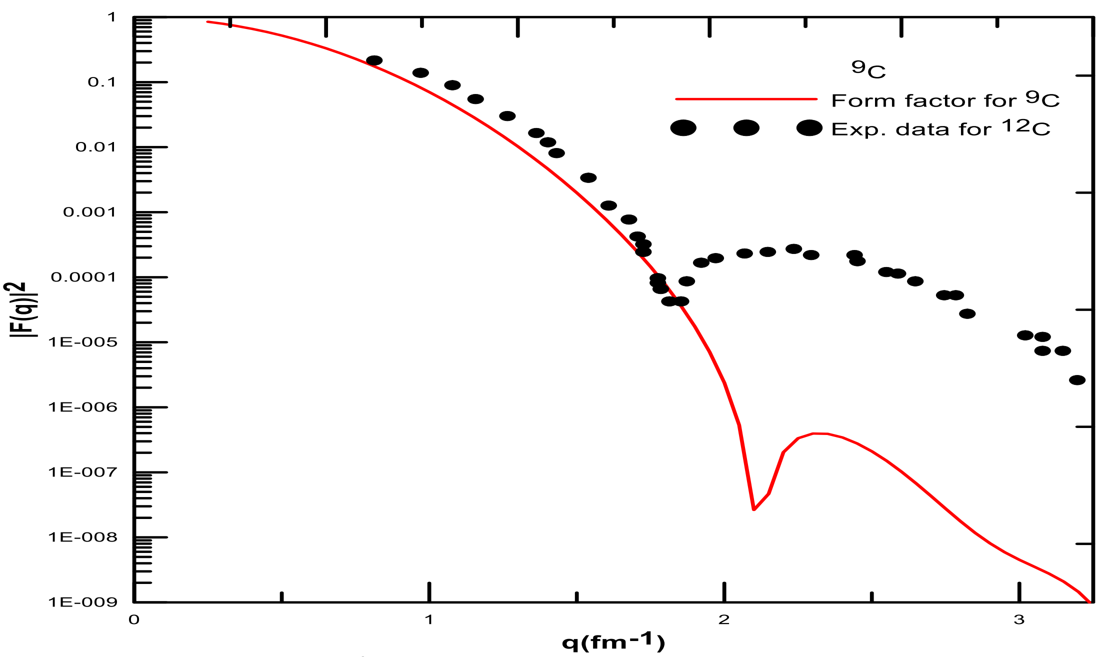

Figure 2: Elastic form factor for ^{9}C nuclei. The filled circle symbols are experimental data [21,22].

Table 1 displays the estimated and observed nucleon rms radii for this nucleus. The experimental results and the theoretically determined rms radii show a high correlation. Fig.3 illustrates the representation of the ground-state 2BNDD in fm^{-3} as a function of r (in fm). The black line, indicating a prolonged tail in this distribution, represents the valence (one proton in the $2s_{1\backslash 2}$ state), whereas the blue line illustrates the core standard contribution. The green line, illustrating the matter density distribution (core + valence), shows an extended tail and aligns well with the experimental data represented by the shaded region.

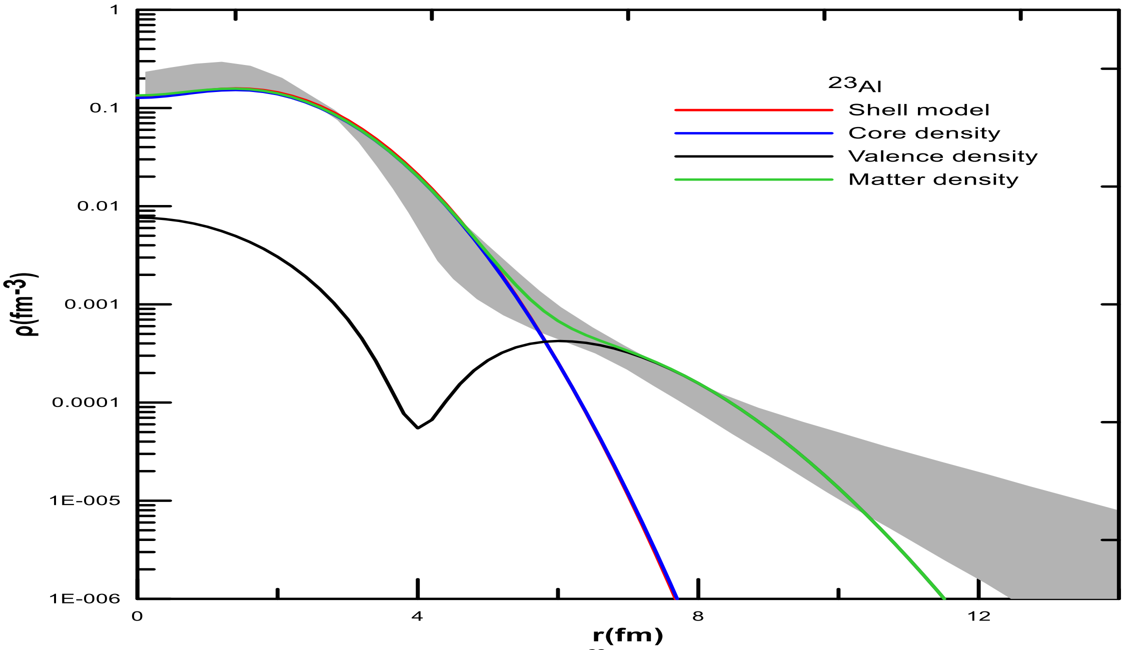

Figure 3: Calculated matter density distribution for ^{23}Al with UCOM parameters compared with the fit to the experimental data [23,24].

The elastic electron scattering form factor is shown in Fig. 4. The red curve represents the theoretically calculated form factor for the nucleus ^{23}Al. At the same time, the black dots correspond to the experimental data for its stable counterpart, ^{27}Al. The calculated form factors for the proton-rich nuclei exhibit distinct behavior, characterized by a significant spatial extension of nucleon distributions, particularly for the valence protons. This extended distribution provides strong evidence for proton-halo structures in these nuclei, in which weakly bound protons occupy orbitals far from the nuclear core. The noticeable deviation between the theoretical form factors and the experimental data for the stable nuclei further supports this interpretation. These findings highlight the importance of incorporating halo effects when modeling the nuclear structure of systems near the proton drip line.

3. 3. ^{27}P Nucleus

The one-proton exotic nucleus ^{27}P has a short half-life of 0.26 seconds. The nucleus (J^π, T= $1/2^+$, 5/2) is formed by connecting the core (J^π, T= 0, +0) with a single valence proton (J^π, T= 1+/2, 5/2). The core oscillator size parameter is b_c = 1.92, yielding an rms radius of 3.11 fm. The valence proton is assumed to occupy a pure ($2s_{1\backslash 2}$) state with an oscillator size parameter of b_v = 3.21 fm, yielding an rms radius of 3.23 fm.

Table 1 displays the estimated and observed nucleon rms radii. The experimental results and the theoretically determined values of rms radii showed good agreement. Fig. 5 illustrates the graph of the ground-state 2BNDD in fm^{-3} as a function of r (in fm). The black line, which shows a long tail in this distribution, represents the valence contribution (one proton in the $2s_{1\backslash 2}$ state), while the blue line represents the core normal contribution. The green line, which represents the matter density distribution (core + valence), has a long tail and closely matches the shaded region, which represents the experimental data.

The elastic electron scattering form factor is shown in Fig.6. The red curve represents the theoretically calculated form factors for nucleus ^{27}P, while the black dots correspond to the experimental data of its stable counterpart ^{31}P. The calculated form factors for the proton-rich nuclei exhibit distinct behavior, characterized by a significant spatial extension of nucleon distributions, particularly for the valence protons.

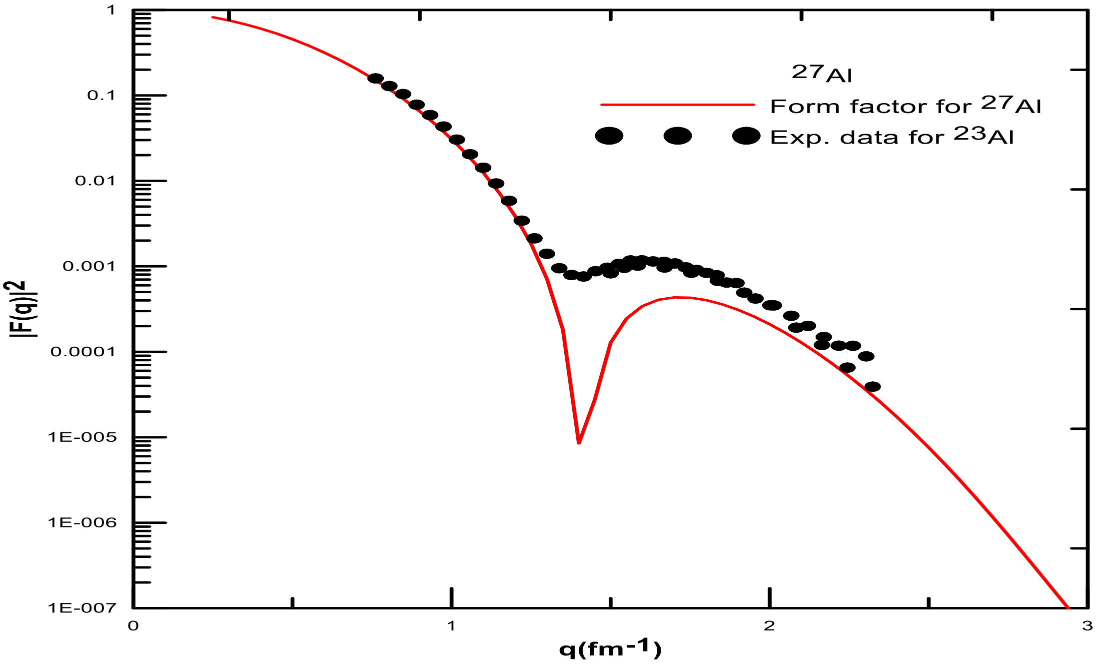

Figure 4: Elastic Form Factor for ^{23}Al nuclei. The filled circle symbols are experimental data [23,24].

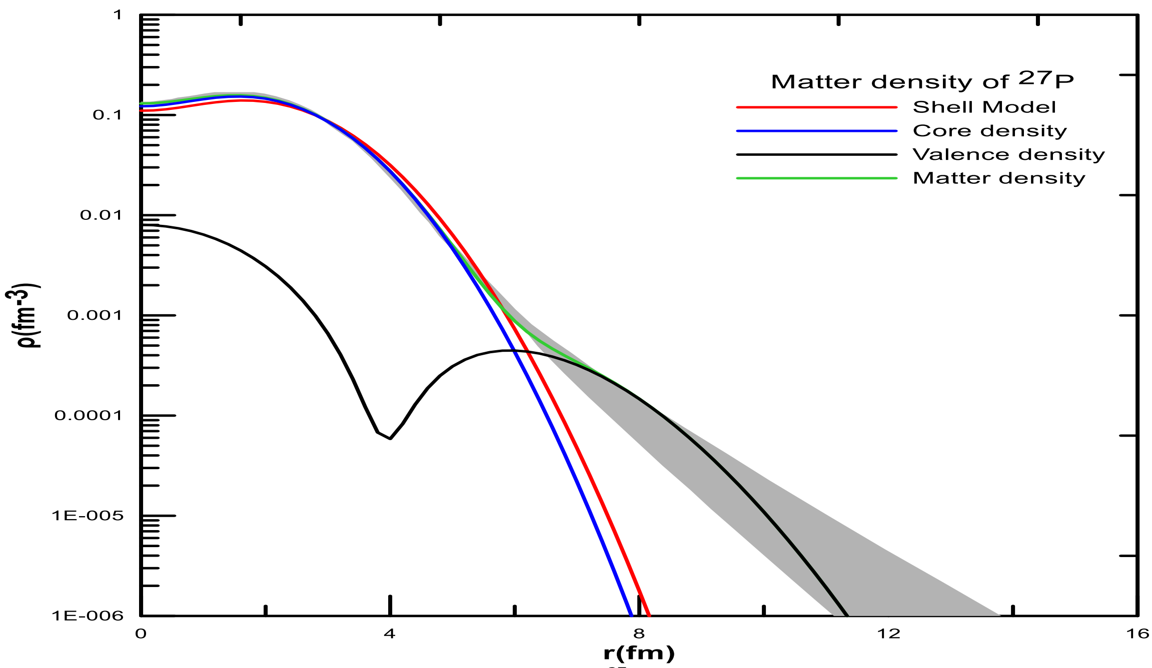

Figure 5: Calculated matter density distribution for ^{27}P with UCOM parameters compared with the fitted circle symbols, which are experimental data [25].

This extended distribution provides strong evidence for the presence of proton-halo structures in these nuclei, where weakly bound protons occupy orbitals far from the nuclear core. The noticeable deviation between the theoretical form factors and the experimental data for the stable nuclei further supports this interpretation. These findings highlight the importance of incorporating halo effects when modeling the nuclear structure of systems near the proton drip line.

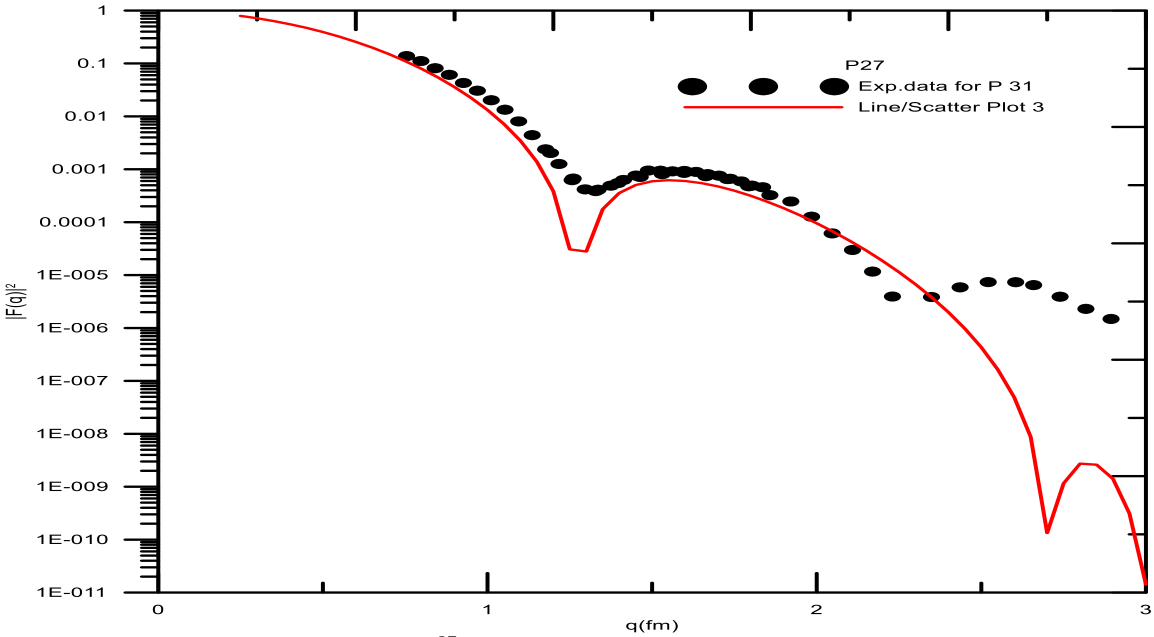

Figure 6: Elastic Form Factor for ^{27}p nuclei. The filled circle symbols are experimental data.

4. Conclusions

In this study, the nuclear structure of exotic nuclei containing a single valence proton, specifically occupying the $2s_{1/2}$ orbital, was analyzed. The matter density of these nuclei exhibited a distinct long-tail behavior, which was investigated through the two-particle correlation coefficient. The results indicate that nuclei containing a single halo proton display structural features that differ significantly from those of stable nuclei. By employing the UCOM, the nucleon distributions and density profiles were accurately described, providing valuable insights into the internal dynamics of these exotic systems. The findings confirm that the two-particle correlation function plays an essential role in enhancing the precision of nuclear structure calculations and in describing proton-neutron interactions. This work contributes to a deeper understanding of the nuclear structure of proton halo systems and demonstrates the effectiveness of the UCOM approach for light exotic nuclei.

Acknowledgements

The authors would like to thank the University of Baghdad, College of Science, Department of Physics, for their assistance in carrying out this work.

Conflict of Interest

The authors declare no conflicts of interest.

References

1. I. Tanihata, H. Savajols, and R. Kanungo, Recent experimental progress in nuclear halo structure studies. *Prog. Part. Nucl. Phys.* **68**, 215 (2013). https://doi.org/10.1016/j.ppnp.2012.07.001.
2. A. N. Antonov, P. E. Hodgson and I. Zh Petkov, *Nucleon momentum and density distributions in nuclei*, Clarendon Press, Oxford (1988).
3. H. G. Benson and B. H. Flowers, A study of deformation in light nuclei: (I). Application to the ground state band of ^{20}Ne and to the low-energy spectrum of 19F. *Nucl. Phys. A.* **126**(2), 305 (1969). https://doi.org/10.1016/0375-9474(69)90468-0.
4. H. Feldmeier, T. Neff, R. Roth and J. Schnack, A unitary correlation operator method. *Nucl. Phys. A.* **632**(1), 61 (1998). https://doi.org/10.1016/S0375-9474(97)00805-1.
5. A. K. Hamoudi, R. A. Radhi and A. R. Ridha, Elastic electron scattering from 17Ne and 27P exotic nuclei, *Iraqi J. Phys.* **13**(28), 68 (2015). https://doi.org/10.30723/ijp.v13i28.244.

6. P. G. Hansen, A. S. Jensen and B. Jonson, Nuclear halos. *Annu. Rev. Nucl. Part. Sci.* **45**, 591 (1995). https://doi.org/10.1146/annurev.ns.45.120195.003111.
7. A. A. Hussein and G. N. Flaiyh, Theoretical study of proton halo structure and elastic electron scattering form factor for 23Al and 27P nuclei by using full correlation functions (tensor force and short range). *East Eur. J. Phys.* **1**, 75 (2023). https://doi.org/10.26565/2312-4334-2023-1-08.
8. H. K. Issa and G. N. Flaiyh, Charge density distributions, elastic and inelastic electron scattering form factors of ^{20}Ne and ^{24}Mg Nuclei. *Iraqi J. Phys.* **23**(1), 20 (2025). https://doi.org/10.30723/ijp.v23i1.1311.
9. T. Neff, and H. Feldmeier, Tensor correlations in the unitary correlation operator method. *Nucl. Phys. A.* **713**(3-4), 311 (2003). https://doi.org/10.1016/S0375-9474(02)01307-6.
10. Z. M. Abbas and G. N. Flaiyh, Study of charge density distributions, elastic and inelastic electron scattering form factors and size radii for ^{19}F and ^{27}Al Nuclei. *Cuestion de Fisioterapia*. **53**(2), 3956 (2024). https://doi.org/10.48047/1m8krv48.
11. R. A. Radhi, A. K. Hamoudi and A. R. Ridha, Elastic electron scattering from unstable neutron-rich P19PC exotic nucleus. *Iraqi J. Sci.* **54**(2), 324 (2013).
12. S. A. Rahi and G. N. Flaiyh, Study of Matter Density Distributions, Elastic electron scattering form factors and Root Mean Square Radii of 9C, 12N, 23Al, 11Be and 15C Exotic Nuclei. *Iraqi J. Sci.* 63(3), 1018 (2022). https://doi.org/10.24996/ijs.2022.63.3.11.
13. R. D. Lawson, *Theory of the Nuclear Shell Model*, Clarendon (Oxford University Press), New York, 1980 https://doi.org/10.1126/science.213.4509.752.a.
14. R. Roth, J. Langhammer, A. Calci, S. Binder and P. Navrátil, Similarity-Transformed Chiral *NN* +3*N* Interactions for the *Ab Initio* Description of ^{12}C and ^{16}O. *Phys. Rev. Lett.* **107**, 072501 (2011). https://doi.org/10.1103/PhysRevLett.107.072501.
15. R. Roth, T. Neff, and F. Hans, Nuclear structure in the framework of the unitary correlation operator method, *Prog. Part. Nucl. Phys.* **65**(1), 50 (2010). https://doi.org/10.1016/j.ppnp.2010.02.003.
16. R. Roth, T. Neff, H. Hergert and H. Feldmeier, Nuclear structure based on correlated realistic nucleon–nucleon potentials. *Nucl. Phys. A* **745**(1-2), 3 (2004). https://doi.org/10.1016/j.nuclphysa.2004.08.024.
17. R. A. Mohammed and W. Z. Majeed, Exotic Structure of 17Ne-17N and 23Al-23Ne Mirror Nuclei. *East Eur. J. Phys.* **4**, 72 (2022). https://doi.org/10.26565/2312-4334-2022-4-05.
18. M. G. Awad and A. R. Ridha, Searching Ground State Properties of some Light Proton-Rich Nuclei Using Whittaker Wave Functions. *in: Journal of Physics: Conference Series, Volume 3028, Technologies and Materials for Renewable Energy, Environment and Sustainability, Casablanca, Morocco.* (2025), 012055. https://doi.org/10.1088/1742-6596/3028/1/012055.
19. S. Q. Abdullah and A. N. Abdullah, Study of the matter density distributions of halo nuclei ^{6}He and ^{16}C using the binary cluster model. *in: 3rd International Conference in Physical Science and Advanced Materials (PAM 2021), Istanbul, Turkey* (2021), **2114**, 012045. https://doi.org/10.1088/1742-6596/2114/1/012045.
20. J. D. Walecka, *Electron scattering for nuclear and nucleon structure*, Cambridge University Press (2001). https://doi.org/10.1017/CBO9780511535017.
21. R. E. Warner, F. Carstoiu, J. A. Brown, F. D. Becchetti, D. A. Roberts¸ B. Davids, A. Galonsky, R. M. Ronningen, M. Steiner, M. Horoi, J. J. Kolata, A. Nadasen, C. Samanta and J. Schwartzenberg, and K. Subotic, Reaction and proton-removal cross sections of ^{6}Li, ^{7}Be, ^{10}B, ^{9,10,11}C, 12N, ^{13,15}O, and ^{17}Ne on Si at 15 to 53 MeV/nucleon. *Phys. Rev. C*, **74**(1), 014605 (2006). https://doi.org/10.1103/PhysRevC.74.014605.
22. Y.-L. Zhao, Z.-Y. Ma, B.-Q. Chen and W.-Q. Shen, Halo Structure of Nucleus 23Al. *Chin. Phys. Lett.* **20**(1), (2003). https://doi.org/10.1088/0256-307X/20/1/316.
23. Z. Y. Lin, M. Z. Yu, C. B. Qiu, Nucleus-Nucleus Scattering Based on a Modified Glauber Theory. *Commun. Theor. Phys.*, **36** (3), 313 (2001). https://ctp.itp.ac.cn/EN/Y2001/V36/I03/313.

دراسة نظرية للتركيب النووي لبعض النوى الغريبة ($^{9}C, ^{23}Al, ^{27}P$) *باستخدام معامل الارتباط الأحادي*

سجى خالد عبد الرزاق [1] وغيث نعمة فليح[1]

[1] قسم الفيزياء، كلية العلوم، جامعة بغداد، بغداد، العراق

الخلاصة

تمّت دراسة البنية النووية لبعض النوى الغريبة أحادية البروتون (C9، Al23، وP27) باستخدام طريقة عامل الارتباط الوحدوي (UCOM). قُسّمت النوى إلى منطقتين: النواة والنيوكليونات التكافؤية. طُبّق تحويل من إطار الجسم الواحد إلى إطار الجسمين، مُدمجًا عامل الارتباط (C)، الذي يُراعي كلاً من ارتباطات الموترات (CΩ) والارتباطات المركزية قصيرة المدى (Cr). حُسبت توزيعات الكثافة لكل منطقة على حدة، وحُدّدت الكثافة الكلية. ومن ذلك، حُسبت القيمة المتوقعة للكثافة، مما أدى إلى تحديد متوسط مربع نصف القطر $\langle r^2\rangle^{1\backslash 2}$. استُخدم تقريب الموجة المستوية بورن (PWBA) لدراسة هذه النوى في حالة تشتت الإلكترونات المرن. بناءً على النتائج المحسوبة، وُجد أن هذا النموذج يُقدّم وصفًا دقيقًا وموثوقًا للبنية النووية لنوى الهالة المدروسة. أظهرت المقارنة بين القيم المحسوبة لمتوسط نصف القطر التربيعي والبيانات التجريبية توافقًا قويًا، مما يؤكد صحة النهج المتبع في وصف بنية نوى الهالة.

الكلمات المفتاحية: النوى الغريبة، توزيع الكثافة، مؤثر الارتباط الاحادي، نصف القطر الجذري التربيعي، تقريب بورن للموجة المستوية.